The American Journal of Human Genetics, Volume *110*

Supplemental information

Rare *EIF4A2* variants are associated with a neurodevelopmental disorder characterized by intellectual disability, hypotonia, and epilepsy

Maimuna S. Paul, Anna R. Duncan, Casie A. Genetti, Hongling Pan, Adam Jackson, Patricia E. Grant, Jiahai Shi, Michele Pinelli, Nicola Brunetti-Pierri, Alexandra Garza-Flores, Dave Shahani, Russell P. Saneto, Giuseppe Zampino, Chiara Leoni, Emanuele Agolini, Antonio Novelli, Ulrike Blümlein, Tobias B. Haack, Wolfram Heinritz, Eva Matzker, Bader Alhaddad, Rami Abou Jamra, Tobias Bartolomaeus, Saber AlHamdan, Raphael Carapito, Bertrand Isidor, Seiamak Bahram, Alyssa Ritter, Kosuke Izumi, Ben Pode Shakked, Ortal Barel, Bruria Ben Zeev, Amber Begtrup, Deanna Alexis Carere, Sureni V. Mullegama, Timothy Blake Palculict, Daniel G. Calame, Katharina Schwan, Alicia R.P. Aycinena, Rasa Traberg, Genomics England Research Consortium, Sofia Douzgou, Harrison Pirt, Naila Ismayilova, Siddharth Banka, Hsiao-Tuan Chao, and Pankaj B. Agrawal

Table S1: **Comparison of epilepsy features and medications used in individuals with *EIF4A2* variants.** This supplemental table compares seizure types and anti-epileptic medications used by each of the individuals with a history of seizures and variants in *EIF4A2.*

Individual	4	5	6	7	8	10	11	12	13	14	15
Collaborator	Carl-Thiem-Klinikum Cottbus, Germany	Manchester Centre for Genomic Medicine	Texas Children's Hospital	Carl-Thiem-Klinikum Cottbus, Germany	Sheba Medical Center, Israel	Cook Children's Hospital, Texas	Federico II University Hospital	Seattle Children's Hospital, Washington	Boston Children's Hospital	Chelsea and Westminster, London, UK	Bambino Gesù Children's Hospital, Rome, Italy
Type of Variant	Compound heterozygous frameshift deletions	Missense	Missense	Compound heterozygous frameshift deletions	Missense	Missense	Missense	Frame shift deletion	Missense	Missense	Missense
cDNA	c.186_187del, c.1161_1166del	c.574G>A	c.481G>T	c.186_187del, c.1161_1166del	c.641C>A	c.647C>T	c.728C>T	c.945_947delCAT	c.1032G>C	c.1084G>A	c.1091G>A
Protein	p.Arg62Serfs*7, p.Asp387_Ile388del)	p.Gly192Ser	p.Gly161Trp	p.Arg62Serfs*7, p.Asp387_Ile388del)	p.Ser214Tyr	p.Thr216Ile	p.Thr243Ile	p.Ile315del	p.Leu344Phe	p.Gly362Ser	p.Gly364Glu
Description of seizures	Myoclonic seizures starting at 1 year	Starting at 3 months of age. Epileptic spasms, tonic seizures with clonic component	Generalized-tonic clonic seizures, onset 19 months	Myoclonic seizures	Intractable myoclonic seizures	Lennox Gastaut Syndrome with tonic seizures and atypical absence seizures	Isolated and cluster spasms, tonic seizures	Focal, well controlled; starting at 3 years	West syndrome with infantile spasms onset at 6 months of age	Starting at 5 months-Infantile spasms and myoclonic seizures, diagnosed with West syndrome; now with tonic, focal, gelastic and absence seizures, diagnosed with Lennox-Gastaut syndrome	EEG at birth showed pathological electrical activity; awaiting additional information
Anti-epileptics	Oxcarbazepine	Levetiracetam, Zonisamide, Clobazam, Cannabidiol March, and Ketogenic diet	Oxcarbazapine, Zonisamide	Lamotrigine, Levetiracetam, Oxcarbazepine, Clobazam, vagus nerve stimulator	Zonisamide, Valproic acid, Pulse steroid, and vagal nerve stimulator	Clobazam and Depakote (partially responsive); plan for trial of ketogenic diet.	Carbamazepine, Brivaracetam, and cannabidiol. The seizure control is sub-optimal and she continues to have frequent seizures.	Previously on Lamotrigine monotherapy with complete control of seizures; after 2 years weaned off medications without return of seizures	Valproic acid, oxcarbamazepine, vigabatrine	Awaiting additional information from clinician	Awaiting additional information from clinician

Table S2: Q5 mutagenesis, sequencing, and qRT-PCR primers and sequences. Table showing all primers used in this study. The mutagenesis primers were used to generate transgenic flies expressing human EIF4A2 WT and variants. Sequencing primers were used for Sanger sequencing to confirm the mutagenesis. Finally, the real-time PCR primers were used to quantify the eIF4A transcript levels due to eIF4A RNAi lines expressed in the GMR-Gal4 domain.

Primer name	Sequence	Purpose
EIF4A2 WT-NS-F	TGACCTTATTGCAAACCCAGCTTTC	To remove stop codon from the WT cDNA
EIF4A2 WT-NS-R	GCCACATTCATGGGCATC	To remove stop codon from the WT cDNA
EIF4A2 p.Gly364Glu-NS-F	ATTGGCAGAGAGGGTCGATTTG	Mutagenesis
EIF4A2 p.Gly364Glu-NS-R	TCTGTGAATATAGTTTTCACGATTG	Mutagenesis
EIF4A2 p.Leu344Phe-NS-F	AAGTGTCTTTCGTTATAAATTATGATC	Mutagenesis
EIF4A2 p.Leu344Phe-NS-R	GTTGCACATCAATCCCGC	Mutagenesis
EIF4A2 p.Thr243Ile-NS-F	GAAGAATTGATCCTTGAAGGAATC	Mutagenesis
EIF4A2 p.Thr243Ile-NS-R	CTTTTTCACCAGAATTCG	Mutagenesis
EIF4A2 p.Thr216Ile-NS-F	CTTTCTGCCATAATGCCAACTG	Mutagenesis
EIF4A2 p.Thr216Ile-NS-R	CAACACAACCTGAATACTTG	Mutagenesis
EIF4A2 SeqP1	GTAAAACGACGGCCAGT	Sequencing
EIF4A2 SeqP2	AATTCTGGCACTTGGAGAC	Sequencing
EIF4A2 SeqP3	ACGAGGCGCAAGGTGGAC	Sequencing
EIF4A2 SeqP4	GTCATAGCTGTTTCCTG	Sequencing
eIF4A-RT-F	GACCGAAATGAGATACCTCAGGA	Real time PCR to check eIF4A mRNA levels
eIF4A-RT-RF	CGCAAGTTCATGTCATCGAAGTT	Real time PCR to check eIF4A mRNA levels
Rps17-RT-F	AAGCGCATCTGCGAGGAG	Endogenous control for real time PCR
Rps17-RT-R	CCTCCTCCTGCAACTTGATG	Endogenous control for real time PCR

Table S3: Statistical summary of one-way ANOVA multiple comparisons for the quantification of total number of misshaped ommatidia. Table showing the *p* value summary for the post-hoc Tukey's multiple comparisons test for different genotypes to compare the total number of misshaped ommatidia.

Tukey's multiple comparisons test	Significant	Summary	Adjusted P value
GMR>empty vs. GMR>UAS dpp	Yes	*	0.0204
GMR>UAS dpp vs. GMR>UAS dpp; UAS eIF4A	No	ns	0.7439
GMR>UAS dpp vs. GMR>UAS dpp; UAS EIF4A2 WT	No	ns	0.1262
GMR>UAS dpp vs. GMR>UAS dpp; p. G364E	Yes	****	<0.0001
GMR>UAS dpp vs. GMR>UAS dpp; p. L344F	Yes	****	<0.0001
GMR>UAS dpp vs. GMR>UAS dpp; p. T243I	Yes	****	<0.0001
GMR>UAS dpp vs. GMR>UAS dpp; p. T216I	No	ns	0.1749
GMR>UAS dpp; UAS eIF4A vs. GMR>UAS dpp; UAS EIF4A2 WT	No	ns	0.9309
GMR>UAS dpp; UAS eIF4A vs. GMR>UAS dpp; p. G364E	Yes	**	0.0055
GMR>UAS dpp; UAS eIF4A vs. GMR>UAS dpp; p. L344F	Yes	***	0.0001
GMR>UAS dpp; UAS eIF4A vs. GMR>UAS dpp; p. T243I	Yes	****	<0.0001
GMR>UAS dpp; UAS eIF4A vs. GMR>UAS dpp; p. T216I	No	ns	0.9486
GMR>UAS dpp; UAS EIF4A2 WT vs. GMR>UAS dpp; p. G364E	No	ns	0.1255
GMR>UAS dpp; UAS EIF4A2 WT vs. GMR>UAS dpp; p. L344F	Yes	**	0.0063
GMR>UAS dpp; UAS EIF4A2 WT vs. GMR>UAS dpp; p. T243I	Yes	***	0.0002
GMR>UAS dpp; UAS EIF4A2 WT vs. GMR>UAS dpp; p. T216I	No	ns	>0.9999

Table S4: Statistical summary of one-way ANOVA multiple comparisons for the quantification of percentage of misshaped ommatidia per field of view. Table showing the *p* value summary for the post-hoc Tukey's multiple comparisons test for different genotypes to compare the percentage of misshaped ommatidia per field of view.

Tukey's multiple comparisons test	Significant	Summary	Adjusted P value
GMR>empty vs. GMR>UAS dpp	Yes	***	0.0005
GMR>UAS dpp vs. GMR>UAS dpp; UAS eIF4A	No	ns	0.2213
GMR>UAS dpp vs. GMR>UAS dpp; UAS EIF4A2 WT	No	ns	0.9997
GMR>UAS dpp vs. GMR>UAS dpp; p. G364E	No	ns	0.1450
GMR>UAS dpp vs. GMR>UAS dpp; p. L344F	Yes	**	0.0033
GMR>UAS dpp vs. GMR>UAS dpp; p. T243I	Yes	**	0.0029
GMR>UAS dpp vs. GMR>UAS dpp; p. T216I	No	ns	0.9991
GMR>UAS dpp; UAS eIF4A vs. GMR>UAS dpp; UAS EIF4A2 WT	No	ns	0.5250
GMR>UAS dpp; UAS eIF4A vs. GMR>UAS dpp; p. G364E	Yes	***	0.0002
GMR>UAS dpp; UAS eIF4A vs. GMR>UAS dpp; p. L344F	Yes	****	<0.0001
GMR>UAS dpp; UAS eIF4A vs. GMR>UAS dpp; p. T243I	Yes	****	<0.0001
GMR>UAS dpp; UAS eIF4A vs. GMR>UAS dpp; p. T216I	No	ns	0.1211
GMR>UAS dpp; UAS EIF4A2 WT vs. GMR>UAS dpp; p. G364E	No	ns	0.0682
GMR>UAS dpp; UAS EIF4A2 WT vs. GMR>UAS dpp; p. L344F	Yes	**	0.0015
GMR>UAS dpp; UAS EIF4A2 WT vs. GMR>UAS dpp; p. T243I	Yes	**	0.0013
GMR>UAS dpp; UAS EIF4A2 WT vs. GMR>UAS dpp; p. T216I	No	ns	0.9755

Table S5: eIF4A LOF rescue assay using human EIF4A2 WT and variants. Table showing cross scheme for rescue analysis and expected genotypes for the lethality rescue flies.

Crosses set up for rescue experiment (at 20-21°C)	Expected genotype
GMR-GAL4/Cyo; UAS empty/TM6B X UAS eIF4A RNAi (VDRC)/Cyo	GMR-GAL4/ UAS eIF4A RNAi (VDRC); UAS empty/+
GMR-GAL4/Cyo; UAS EIF4A2 WT/TM6B X UAS eIF4A RNAi (VDRC)/Cyo	GMR-GAL4/ UAS eIF4A RNAi (VDRC); UAS EIF4A2 WT/+
GMR-GAL4/Cyo; UAS EIF4A2 p.Gly364Glu/TM6B X UAS eIF4A RNAi (VDRC)/Cyo	GMR-GAL4/ UAS eIF4A RNAi (VDRC); UAS EIF4A2 p.Gly364Glu/+
GMR-GAL4/Cyo; UAS EIF4A2 p.Leu344Phe/TM6B X UAS eIF4A RNAi (VDRC)/Cyo	GMR-GAL4/ UAS eIF4A RNAi (VDRC); UAS EIF4A2 p.Leu344Phe/+
GMR-GAL4/Cyo; UAS EIF4A2 p.Thr243Ile/TM6B X UAS eIF4A RNAi (VDRC)/Cyo	GMR-GAL4/ UAS eIF4A RNAi (VDRC); UAS EIF4A2 p.Thr243Ile/+
GMR-GAL4/Cyo; UAS EIF4A2 p.Thr216Ile/TM6B X UAS eIF4A RNAi (VDRC)/Cyo	GMR-GAL4/ UAS eIF4A RNAi (VDRC); UAS EIF4A2 p.Thr216Ile/+

Supplementary Figure S1: Molecular modelling of EIF4A2 variants. (A) Overall structural model of EIF4A2 with protein in green, nucleic acid in blue. The affected residues are colored in red. **(B)** Magnified regions of affected residues. **(i-ii)** The pathogenic variant p.Ser214Tyr is important for NTD-CTD interaction. **(iii-iv)** p.Gly362Ser destabilizes the local helix. **(v-vi)** p.Gly192Ser increases the physical interaction between EIF4A2 and the nucleic acid.

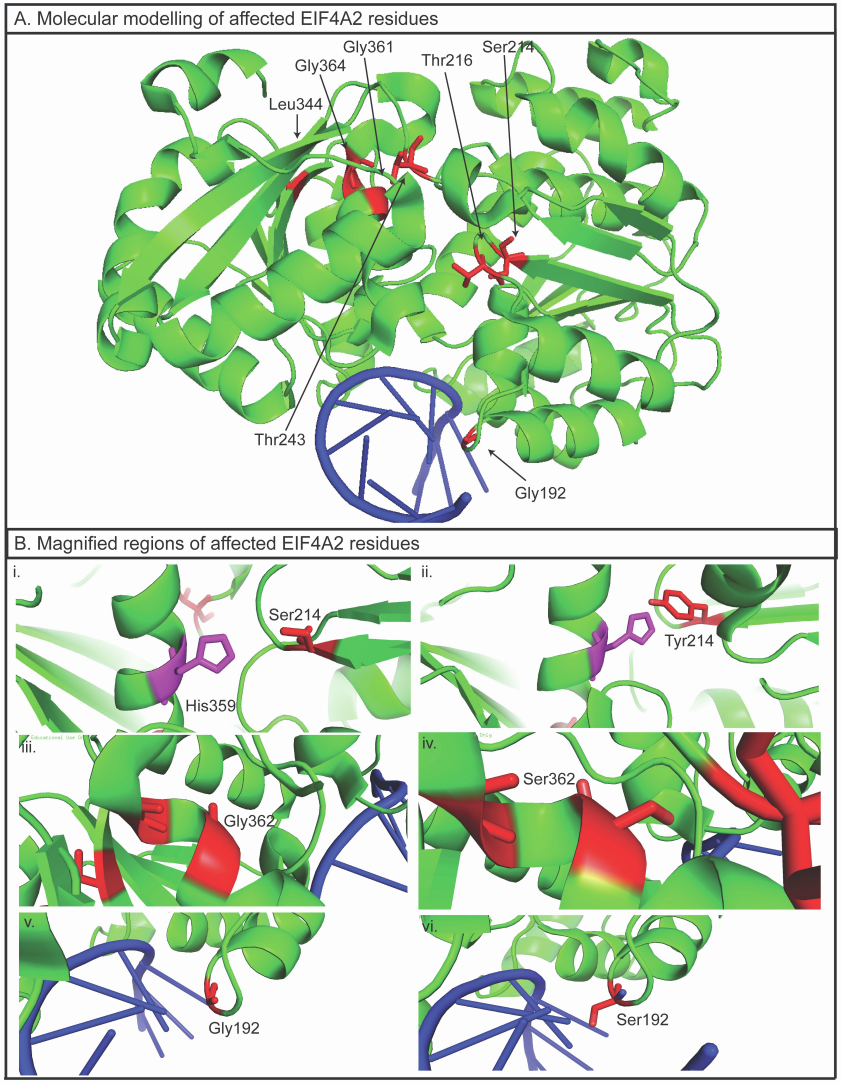

Supplementary Figure S2: pMad expression in Nubbin-GAL4 driven wing discs overexpressing eIF4a or EIF4A2 WT and variants. (A) Representative third instar larval wing imaginal discs are shown with pMad (green, arrow marks the pMad expression in wing pouch) and HA (magenta, HA marks the NubGAL4 expression area). **(B)** Quantification of pMad fluorescence intensity in the wing disc pouch (HA expression area) shows that Nubbin-GAL4 mediated expression of eIF4a and EIF4A2 p.Thr216Ile causes reduced pMad expression compared to empty control. Data shown as mean ± standard error of mean (SEM) with the sample size of total number of larvae shown in figure. Significance shown as *p<0.05. **(C)** Representative images of Nubbin-GAL4 driven adult wings are shown for empty, eIF4a, and EIF4A2 p.Thr216Ile. Reduced wing size, blisters (asterisk), and wing margin serration (arrow) are observed for both eIF4a and EIF4A2 p.Thr216Ile.

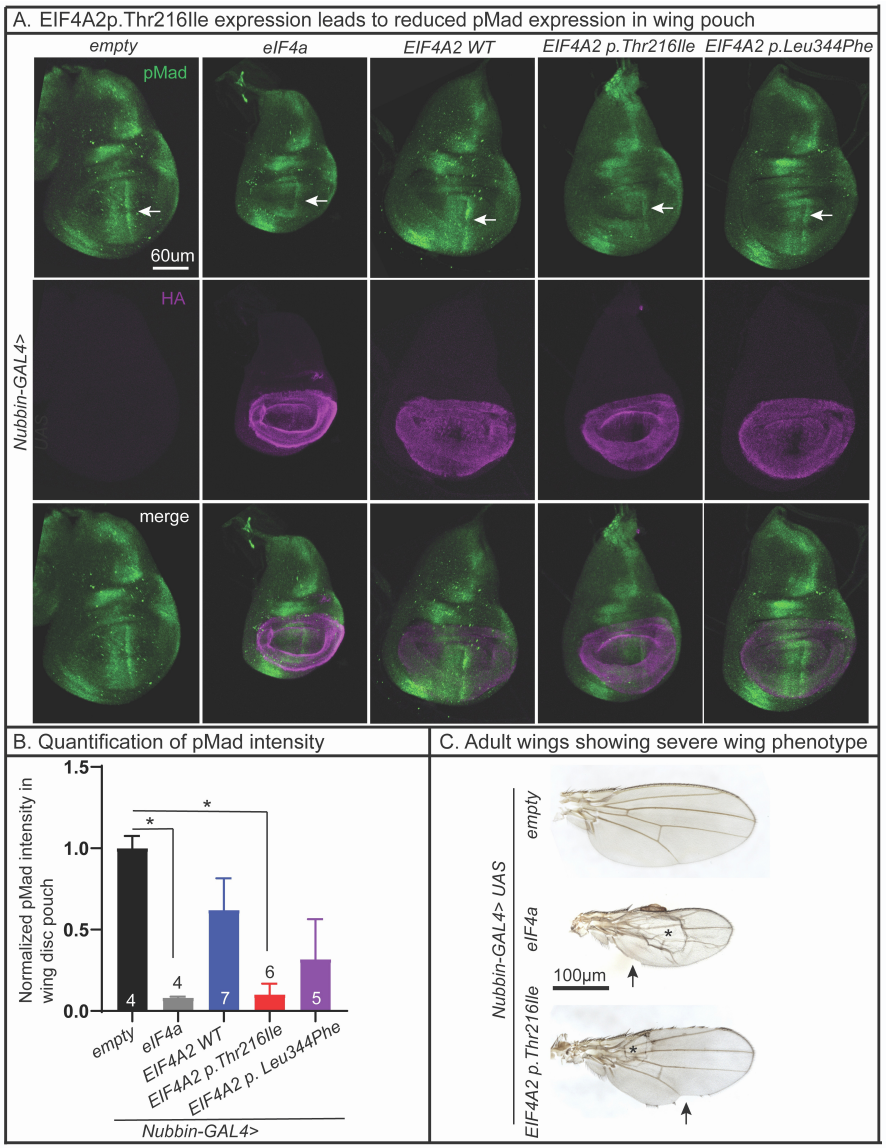

Supplementary Figure S3: RNAi mediated knockdown of eIF4A. **(A)** GMR-GAL4 and nubbin-GAL4 mediated knock down of two different eIF4A RNAi lines (BDSC#33970 and VDRC#42201) at 25°C and 20°C resulted in either embryonic or pupal lethality. **(B)** eIF4A transcripts are found to be significantly reduced in GMR-GAL4 driven eIF4A RNAi lines. Pharate adult head was used to collect RNA and the crosses were set at room temperature. One-way ANOVA followed by Tukey's post-hoc test was performed for the statistical analysis. Data shown mean ± SEM with sample size of biological replicates of pooled male and female flies shown in figure. Significance shown as ****p<0.0001.

A. eIF4A RNAi mediated knock down results in embryonic and pupal lethality

Temperature	25C		20C
RNAi line	GMR GAL4	nubbin GAL4	GMR GAL4
luciferase RNAi	adult viable	adult viable	adult viable
eIF4A RNAi (BDSC)	late pupal lethal	late pupal lethal	late pupal lethal
eIF4A RNAi (VDRC)	embryonic lethal	embryonic lethal	late pupal lethal

B. Reduced eIF4A transcripts in eIF4A RNAi lines

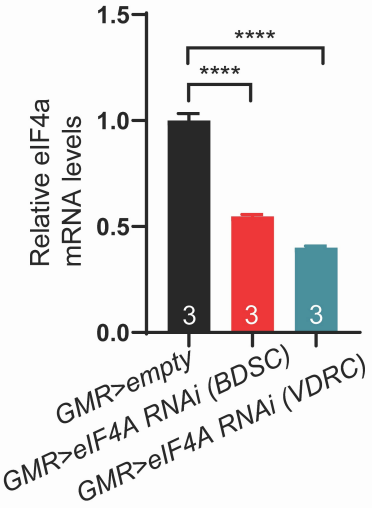

n = 10 pharate male and female heads per biological replicate

Crosses set at 20-21C

BDSC#33970
VDRC#42201

**** p<0.0001
1-ANOVA with Tukey's post-hoc

ACKNOWLEDGEMENTS

We thank the families and clinical staff at each location for participation in this study. The P.B.A's research work is supported by the National Institute of Arthritis and Musculoskeletal and Skin Diseases, R01AR068429-01, National Human Genome Research Institute, 1R01HG011798-01A1 and "Because of Bella" foundation. H.T.C. is funded from the McNair Medical Institute at Robert and Janice McNair Foundation, Child Neurology Foundation and Society, The Gordon and Mary Cain Foundation, Annie and Bob Graham, The Elkins Foundation, and the Mark A. Wallace Endowment Award. M.S.P.'s research effort is supported in part by the National Ataxia Foundation and the Burroughs Wellcome Fund. A.R.D.'s research effort was supported by the National Institutes of Health, T32HD098061. D.G.C.'s research effort was supported by Muscular Dystrophy Association Development Grant 873841 (https://doi.org/10.55762/pc.gr.147552), Chao Physician-Scientist Award, and 5T32GM007526 Medical Genetics Research Program. This work was supported in part by the Manton Center for Orphan Disease Research and Sanger sequencing performed by the Boston Children's Hospital IDDRC Molecular Genetics Core Facility supported by NIH award U54HD090255 from the National Institute of Child Health and Human Development. Sequencing and analysis for individual 12 was provided by the Broad Institute of MIT and Harvard Center for Mendelian Genomics (Broad CMG) and was funded by the National Human Genome Research Institute, the National Eye Institute, and the National Heart, Lung and Blood Institute grant UM1 HG008900 and in part by National Human Genome Research Institute grant R01 HG009141. This work was also supported by the Strasbourg's Interdisciplinary Thematic Institute (ITI) for Precision Medicine, TRANSPLANTEX NG, as part of the ITI 2021-2028 program of the University of Strasbourg, CNRS and INSERM, funded by IdEx Unistra [ANR-10-IDEX-0002] and SFRI-STRAT'US [ANR-20-SFRI-0012]. This work was supported by Fondazione Telethon, Telethon Undiagnosed Diseases Program (TUDP, GSP15001). This research was supported by the National Institute for Health Research (NIHR) Oxford Biomedical Research Centre Programme and the Wellcome Trust (203141/Z/16/Z). This research was made possible through access to the data and findings generated by the 100,000 Genomes Project. The 100,000 Genomes Project is managed by Genomics England Limited (a wholly owned company of the Department of Health and Social Care). The 100,000 Genomes Project is funded by the National Institute for Health Research and NHS England. The Wellcome Trust, Cancer Research UK and the Medical Research Council have also funded research infrastructure. The 100,000 Genomes Project uses data provided by individuals and collected by the National Health Service as part of their care and support. A.J. is supported by Solve-RD. The Solve-RD project has received funding from the European Union's Horizon 2020 research and innovation program under grant agreement No 779257. This study was in parts generated within the European Reference Network ITHACA. E.A. and A.N. are supported by Ricerca Corrente 2021, Ministero della Salute. T.B.H. was supported by the Deutsche Forschungsgemeinschaft (DFG, German Research Foundation) – 418081722, 433158657. The study was supported by the German Feral Ministry of Education and Research (BMBF, Bonn, Germany) through the German Network for Mitochondrial Disorders (mitoNET, 01GM1906D). B.A. is supported by the German Federal Ministry of Education and Research (BMBF) within the framework of the e:Med research and funding concept (grant #FKZ 01ZX1405C), through the German Network for mitochondrial disorders (mitoNET, 01GM1906D). We thank Drs. Hugo Bellen and Hamed Jafar-Nejad for providing *Drosophila melanogaster* stocks.